The American Journal of Pathology, Vol. 183, No. 4, October 2013

The American Journal of
PATHOLOGY
ajp.amjpathol.org

IMMUNOPATHOLOGY AND INFECTIOUS DISEASES

# HSV-1 Targets Lymphatic Vessels in the Eye and Draining Lymph Node of Mice Leading to Edema in the Absence of a Functional Type I Interferon Response

Katie M. Bryant-Hudson, Ana J. Chucair-Elliott, Christopher D. Conrady, Alex Cohen, Min Zheng, and Daniel J.J. Carr

*From the Department of Ophthalmology, University of Oklahoma Health Sciences Center, Oklahoma City, Oklahoma*

Accepted for publication June 20, 2013.

Address correspondence to Daniel J.J. Carr, Ph.D., Department of Ophthalmology, Dean McGee Eye Institute, Room 415, The University of Oklahoma Health Sciences Center, 608 Stanton L Young Boulevard, Oklahoma City, OK 73104. E-mail: dan-carr@ouhsc.edu.

Herpes simplex virus type-1 (HSV-1) induces new lymphatic vessel growth (lymphangiogenesis) in the cornea via expression of vascular endothelial growth factor by virally infected epithelial cells. Here, we extend this observation to demonstrate the selective targeting of corneal lymphatics by HSV-1 in the absence of functional type I interferon (IFN) pathway. Specifically, we examined the impact of HSV-1 replication on angiogenesis using type I IFN receptor deficient ($CD118^{-/-}$) mice. HSV-1-induced lymphatic and blood vessel growth into the cornea proper was time-dependent in immunocompetent animals. In contrast, there was an initial robust growth of lymphatic vessels into the cornea of HSV-1-infected $CD118^{-/-}$mice, but such vessels disappeared by day 5 postinfection. The loss was selective as blood vessel integrity remained intact. Magnetic resonance imaging and confocal microscopy analysis of the draining lymph nodes of $CD118^{-/-}$ mice revealed extensive edema and loss of lymphatics compared with wild-type mice. In addition to a loss of lymphatic vessels in $CD118^{-/-}$ mice, HSV-1 infection resulted in epithelial thinning associated with geographic lesions and edema within the cornea, which is consistent with a loss of lymphatic vasculature. These results underscore the key role functional type I IFN pathway plays in the maintenance of structural integrity within the cornea in addition to the anti-viral characteristics often ascribed to the type I IFN cytokine family. *(Am J Pathol 2013, 183: 1233–1242; http://dx.doi.org/10.1016/j.ajpath.2013.06.014)*

The primary function of the lymphatic system is to drain fluid and macromolecules from peripheral tissue and return them to the blood circulation to maintain appropriate peripheral tissue pressure.[1] Antigen, antigen-presenting cells, and soluble factors drain from the site of inflammation to the regional lymph nodes (LNs).[1] This process is due to structural differences between blood and lymphatic capillaries. The endothelial cells of blood capillaries form tight junctions are surrounded by a basement membrane and by vascular smooth muscle cells,[1] whereas lymphatic capillaries are composed of a single layer of endothelial cells connected loosely by button-like junctions that facilitate the uptake of $CCR7^{+}$ immune cells via CCL21 expression by lymphatic endothelial cells (LECs).[2] Therefore, the lymphatic system plays a crucial role bridging the innate immune response at the site of inflammation to the generation of an adaptive immune response in the draining LN. However, under pathological conditions lymphangiogenesis or the impairment of proper lymphatic drainage can contribute to tumor metastasis, chronic inflammation, or lymphedema. Blood and lymphatic vessels are critical for tissue maintenance; however, certain tissues, such as the central cornea, are avascular. The absence of blood and lymphatic vessels in the cornea is necessary for visual acuity. However, hemangiogenesis and lymphangiogenesis can occur after inflammation or transplantation. With the identification of novel lymphatic vessel markers [lymphatic vessel endothelial hyaluronan receptor 1 (LYVE-1), prospero homeobox 1 (Prox1), and podoplanin], corneal lymphangiogenesis has been investigated using wound healing and corneal transplantation models. In these studies, corneal

Supported in part by NIH grant EY021238 (D.J.J.C.), the OUHSC Presbyterian Health Foundation Presidential Professorship and Research to Prevent Blindness Senior Investigator awards (D.J.J.C.), an National Eye Institute Core grant P30 EY12190, and an National Institute of Allergy and Infectious Diseases training grant AI007633 (K.M.B.-H.).

K.M.B.-H., A.J.C.-E., and C.D.C. contributed equally to this work.


http://dx.doi.org/10.1016/j.ajpath.2013.06.014

lymphangiogenesis was associated with hemangiogenesis contributed by inflammatory cells through vascular endothelial growth factor (VEGF)-C/VEGF receptor 3 signaling.[3] The presence of lymphatic vessels in the cornea before transplantation significantly reduced graft success via the trafficking of graft antigens to the regional LNs.[3] Moreover, excision of the draining LNs before transplantation increased graft survival to 90%, even under high-risk settings.[4]

Herpes simplex virus type-1 (HSV-1) is among the most successful of human pathogens with a seroprevalence rate between 50% to 80%.[5] Regardless of treatment, infection is lifelong due to the virus establishing a latent infection in sensory neurons, thereby evading immune detection.[6] On reactivation, the virus replicates and travels by anterograde transport to the primary site of infection or other epithelial surfaces fed by the infected sensory nerve fibers.[6] The most common clinical manifestation of HSV-1 infection is orolabial lesions; however, the virus can also be transported to the cornea resulting in recurring bouts of inflammatory keratitis.[7] The clinical signs of herpes stromal keratitis include stromal opacity, edema, and neovascularization.[7] The occurrence of corneal edema is believed to allow for easier growth of new vessels between collagen lamellae.[8] Recent studies have highlighted the importance of DNA sensor IFI-16/p204-driven type 1 interferon (IFN) signaling by infected corneal epithelial cells in controlling viral replication through the recruitment of inflammatory monocytes.[9,10]

The development of lymphatic vessels into the central cornea after ocular HSV-1 infection has been described recently.[11] Ocular infection with HSV-1 was found to elicit resident epithelial cell expression of the pro-lymphangiogenic factor, VEGF-A, in the cornea that required binding of the HSV-1 encoded immediate to early transcription factor, ICP4, to Sp1 sites within the *VEGF*-A promoter.[12] Subsequent release of VEGF-A by HSV-1−infected corneal epithelial cells during acute infection is thought to lead to robust lymphangiogenesis in the cornea proper, preceding the development of blood vessels.[11] It has also been noted that HSV-1 drives vascularization of the cornea by reducing the expression of soluble VEGFR1, which functions as a VEGF-A trap, blocking any downstream signaling.[13]

We show that impairment of type 1 IFN signaling results in extensive corneal edema and loss of epithelial layers due to robust replication of the virus within the tissue and skewed leukocyte recruitment pattern. Moreover, HSV-1 selectively targets lymphatic vessels, but not blood vessels during acute infection in both the cornea and draining LN.

## Materials and Methods

### Mice, Cells, and HSV-1 Infection

C57BL/6 wild-type (WT) mice were obtained from The Jackson Laboratory (Bar Harbor, ME). C57BL/6 congenic CD45.1 mice were obtained from National Cancer Institute (Frederick, MD). Mice deficient in the type I IFN receptor α chain (*CD118*$^{-/-}$ mice)[14] on a WT CD45.2 background were maintained at Dean McGee Eye Institute (Oklahoma City, OK). Animal treatment was consistent with the National Institutes of Health Guidelines on the Care and Use of Laboratory Animals. All procedures were approved by the University of Oklahoma Health Sciences Center and Dean McGee Eye Institute Institutional Animal and Care and Use Committee. To establish infection, HSV-1 (strain McKrae) or green fluorescent protein (GFP)-expressing HSV-1[15] were used to infect age- and sex-matched mice as previously described.[9] HSV-1 viral titers were determined in the designated tissue at postinfection (p.i.) times by plaque assay. Blood endothelial cell (BEC) and LEC (ATCC, Manassas, VA) co-cultures were infected with GFP-expressing HSV-1 at a multiplicity of infection of 5 for 24 hours.

### Slit-Lamp Examination of the Corneas

At indicated times p.i. with $10^3$ PFU of HSV-1 (McKrae strain), a Micron III imaging platform with a slit-lamp attachment (Phoenix Research Laboratories, Pleasanton, CA) was used for anterior segment imaging of anesthetized, HSV-1-infected WT, and *CD118*$^{-/-}$ mice with a slit beam. To visualize the corneal epithelial integrity, the corneas of infected WT and *CD118*$^{-/-}$ mice were treated with topical sodium fluorescein (Wilson Ophthalmic, Mustang, OK) and images captured under cobalt illumination, using the Micron III system (Phoenix Research Laboratories).

### Measurement of Corneal Thickness and Weight

As previously described,[16] an ultrasound pachymeter (CorneoGage Plus; Sonogage, Cleveland, OH) that allowed perpendicular alignments between the probe and central cornea was used for central corneal thickness measurements of anesthetized uninfected and infected WT and *CD118*$^{-/-}$ mice at the indicated time p.i., as suggested by the manufacturer. After these experiments, a group of infected WT and *CD118*$^{-/-}$ mice were euthanized on days 3 and 4 p.i., and their corneas were dissected at the margin of the limbus, blotted with tissue paper, and weighed for comparison.

For histological assessment of corneal thickness, uninfected and infected WT and *CD118*$^{-/-}$ whole eyes were harvested at the indicated time p.i. The eyes were then fixed for 24 hours at room temperature and transferred to 70% ethanol. After paraffin embedding, 5 μm sections were mounted on slides and stained with H&E. Images were then captured with a Nikon (Melville, NY) Eclipse E800 epifluorescence microscope, and the number of epithelial layers and total corneal thickness were measured in representative central areas.

### Flow Cytometry

Leukocyte infiltration into the cornea proper or residing in the mandibular lymph nodes (MLN) of uninfected and infected mice was performed as previously described.[10]

### Bone Marrow Chimeras

Bone marrow chimeras were created by irradiating WT CD45.2 and *CD118*$^{-/-}$ CD45.1 mice with two 600-Gy doses of γ-irradiation spaced 4 hours apart. Irradiated mice were then retro-orbitally injected with $3 \times 10^6$ bone marrow cells from WT or *CD118*$^{-/-}$ mice. The injected bone marrow cells were allowed 10 weeks to reconstitute the hematopoietic compartment. Chimerism was verified by flow cytometry on circulating leukocytes in which recipients were found to be composed of 90% to 95% donor bone marrow cells.

### Immunofluorescence Microscopy and Quantitative Analysis of Lymphangiogenesis

Corneas from infected and uninfected mice were removed and processed as previously described.[11] MLN were prepared and stained for specific antigens as previously described.[17] MLN images were obtained with a 10× objective and aggregated using Photoshop CS4 (Adobe Systems, Inc., San Jose, CA) to visualize whole LNs. LYVE-1 expression was quantified as previously described using MetaMorph Imaging Suite version 7.7 (Molecular Devices Inc., Sunnyvale, CA).[11] Human BEC and LEC were fixed and imaged in the same manner as cornea samples, except the cells were stained with anti-Prox1 primary antibodies. To quantify HSV-1 infection of BEC and LEC 24 hours p.i., cells positive for GFP (indicating HSV-1 infection) in the visual field were counted using a masked observer. BEC/LEC images were obtained with a 200× objective. Cells positive for Prox1 (indicating LEC) or negative for Prox1 (indicating BEC) in the same visual field were counted and total cells (indicated by DAPI stain) were enumerated. The number of cells counted was then compared with the total number of cells in each visual field to calculate percentage of HSV-1 positive cells. All samples were imaged using an Olympus IX81-FV500 epiflourescence/confocal laser-scanning microscope (Olympus, Center Valley, PA). Images were analyzed with Fluoview software (Olympus).

### Magnetic Resonance Imaging

WT and *CD118*$^{-/-}$ mice were subjected to gas anesthesia (1.5% to 2.5% isoflurane, 0.8 L/min $O_2$). At the indicated time p.i., mice were imaged using a Bruker Biospec 5.0 imaging system to capture T2-weighted images. Areas of fluid accumulation were calculated by drawing regions of interest around the pharyngeal region that were then analyzed using Paravision software version 5.0.

### Suspension Array and Real-Time PCR

At the indicated p.i. time, mice were euthanized and corneas were harvested, processed, and evaluated for CXCL1, CXCL-9, and CXCL-10, or VEGF-A (Millipore, Billerica, MA) by a Bioplex suspension array system (BioRad, Hercules, CA) as previously described.[18] VEGF-C was measured by ELISA (eBiosciences Rat VEGF-C ELISA Kit; Bender MedSystems Gmbh, Vienna, Austria) according to the manufacturer's instructions. The weight of each tissue was used to normalize the amount of cytokine/chemokine per milligram of tissue weight.

For real-time RT-PCR, corneas were harvested and mRNA was isolated and converted into cDNA as previously described.[11] The abundance of VEGF-A, VEGF-C, and VEGF-D cDNA relative to the housekeeping gene β-actin was calculated as $2^{-\Delta\Delta Ct}$.

### Statistical Analysis

The statistical module Prism version 5.0 (GraphPad Software, Inc., San Diego, CA) was used to perform unpaired two-tailed Student's *t*-test with group sizes of two or analysis of variance with Tukey's *t*-test for larger group sizes. Where indicated, outliers were identified and removed using a Grubbs' test.

## Results

### Loss of IFN Signaling Results in Substantial Corneal Pathology after HSV-1 Infection

Type I IFN production elicited by HSV-1 driven IFI16/p204 sensor activation in corneal epithelial cells is critical for virus surveillance.[10] Still, how the type I IFN pathway regulates tissue pathology in the cornea is not understood. To profile the corneal pathology during acute HSV-1 infection in the absence of IFN signaling, WT and *CD118*$^{-/-}$ mice were infected with HSV-1 and their corneas were subjected to pathology assessment.

Slit-lamp examination on day 5 p.i. revealed that *CD118*$^{-/-}$ mice presented with complete opacification of their corneas associated with stromal keratitis and haze, and minimal visible anterior chamber and iris details (Figure 1A). In comparison, their WT counterparts showed faint corneal scars and clear irises, indicating a rather translucent cornea outside of the area of the scar (Figure 1A). Slit-lamp imaging on days 4 and 5 p.i. revealed a loss of the corneal epithelium integrity, as shown by almost complete fluorescein staining of the corneal surface of *CD118*$^{-/-}$ mice (Figure 1B) compared with the infected WT cornea (Figure 1B). Consistent with this finding, *CD118*$^{-/-}$ mice had >30% increase in central corneal thickness as measured by pachymetry on days 3 and 4 p.i. (Figure 1C) and a significant increase in corneal mass on day 3 p.i. (Figure 1D) compared with the infected WT counterparts. Histological analysis revealed a loss of epithelial layers of the infected cornea of *CD118*$^{-/-}$ mice on days 3 and 5 p.i. with increased overall corneal thickness on day 5 p.i. (Figure 2, A–D). Such epithelial cell loss was inversely correlated with the content of infectious virus recovered from *CD118*$^{-/-}$ mouse corneas (Figure 2E).

HSV-1 infection of the cornea results in leukocyte infiltration, including monocytes, macrophages, neutrophils, and

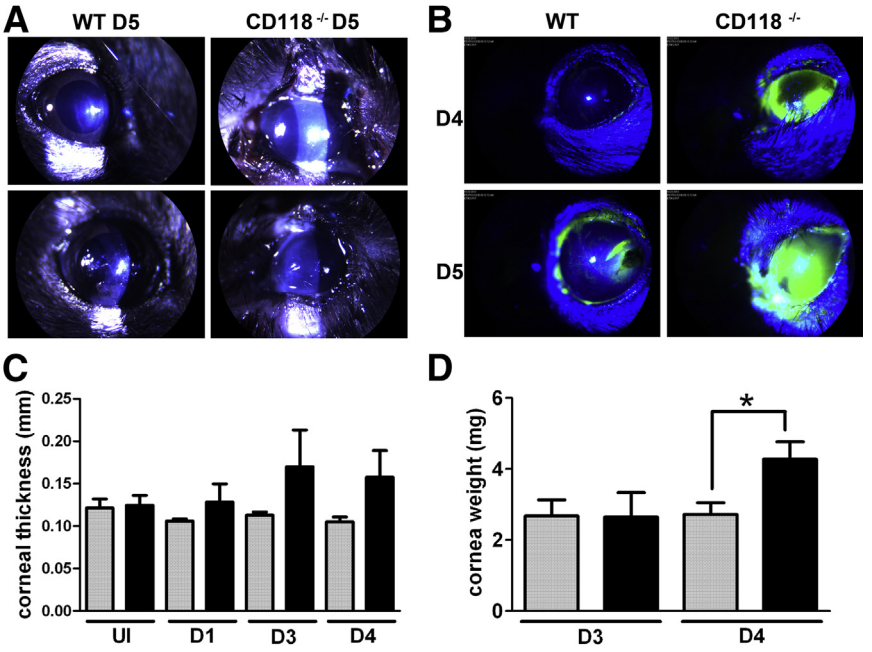


**Figure 1** Loss of type I IFN signaling predisposes mice to extensive corneal pathology including the development of edema and loss of epithelial integrity after HSV-1 infection. **A:** Representative slit-lamp images of two *CD118*$^{-/-}$ and two WT mice on day 5 p.i. (D5) with $10^3$ PFU of HSV-1. **B:** Representative slit-lamp images of *CD118*$^{-/-}$ and WT corneas topically stained with fluorescein dye on days 4 and 5 p.i. (D4 and D5, respectively) with $10^3$ PFU of HSV-1. **C:** Pachymetry measurements of corneal thickness comparing uninfected (UI) and infected WT (grey bars) and *CD118*$^{-/-}$ (black bars) mice. **D:** Comparison between cornea weight of WT (grey bars) and *CD118*$^{-/-}$ (black bars) mice on days 3 and 4 p.i. (D3 and D4, respectively) with $10^3$ PFU of HSV-1. By day 4 p.i., *CD118*$^{-/-}$ had >30% increased weight compared to the WT group. The values are presented as the means ± SEM from three corneas per time point group. *$P < 0.05$ comparing WT with *CD118*$^{-/-}$ by unpaired *t*-test comparison.

natural killer (NK) cells.[19–21] To compare the phenotype of the innate immune response in the HSV-1-infected *CD118*$^{-/-}$ with WT mouse corneas, flow cytometry analysis was performed. On days 3 and 5 p.i., *CD118*$^{-/-}$ mouse corneas contained fewer NK cells (Figure 3A), as well as inflammatory monocytes (Figure 3B), compared with infected WT mouse cornea samples. By day 5 p.i., the macrophage infiltrate was nearly absent in the *CD118*$^{-/-}$ mouse corneas (Figure 3C), whereas there was a significant increase in the number of neutrophils (Figure 3D). No significant change in the number of total leukocytes (defined as CD45$^{Hi}$) was observed (Figure 3E).

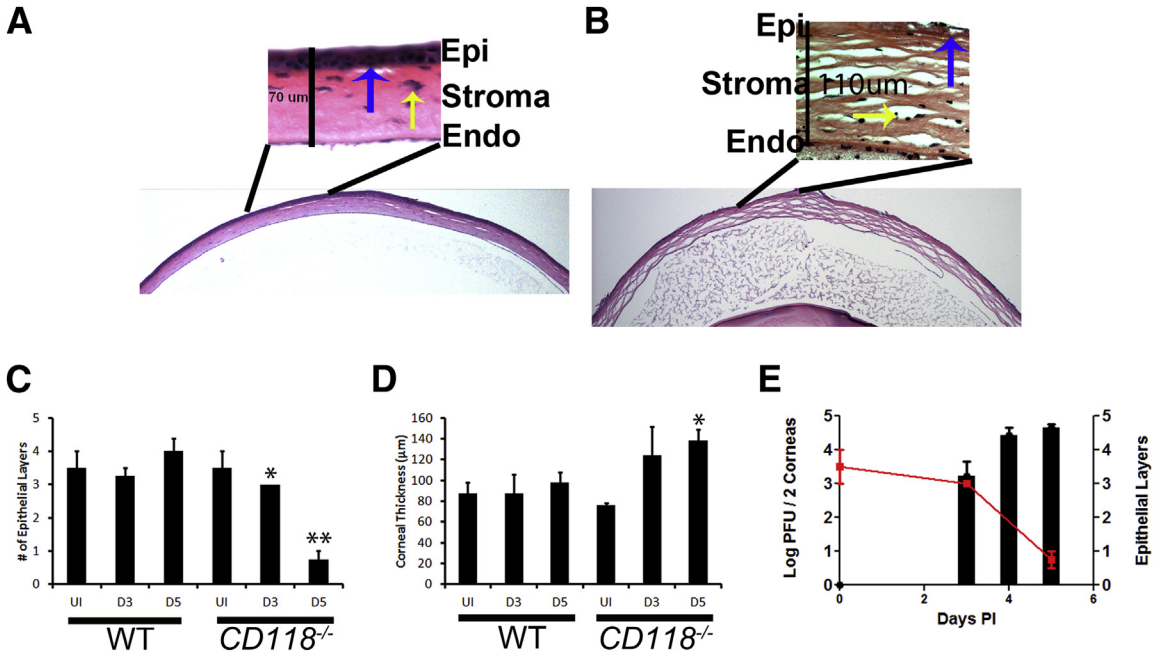


**Figure 2** CD118 deficiency results in histological and pathological findings and epithelial loss. WT and *CD118*$^{-/-}$ mice were ocularly infected with $10^3$ PFU of HSV-1 or remained uninfected (UI) as controls. Eyeballs were collected at days 3 and 5 p.i. (D3 and D5, respectively), fixed, and processed for histology. Representative images of H&E stained cross sections of the eye of WT infected (**A**) and *CD118*$^{-/-}$ infected (**B**) corneas on day 5 p.i. The number of corneal epithelial layers (**C**) and corneal thickness (**D**), both in *CD118*$^{-/-}$ and WT mice, were each quantified using images captured from H&E histological sections as show in **A** and **B**. **E:** Quantitative correlation between the viral content (black bars) and the number of corneal epithelial layers (**red line**) assessed by plaque assay and histological measurements, respectively, in *CD118*$^{-/-}$ corneas at the indicated time points p.i. Results are presented as the means ± SEM of two to three experiments per group of two to four eyes per group per experiment. *$P < 0.05$, **$P < 0.01$ comparing WT with *CD118*$^{-/-}$ mice by unpaired *t*-test comparison.

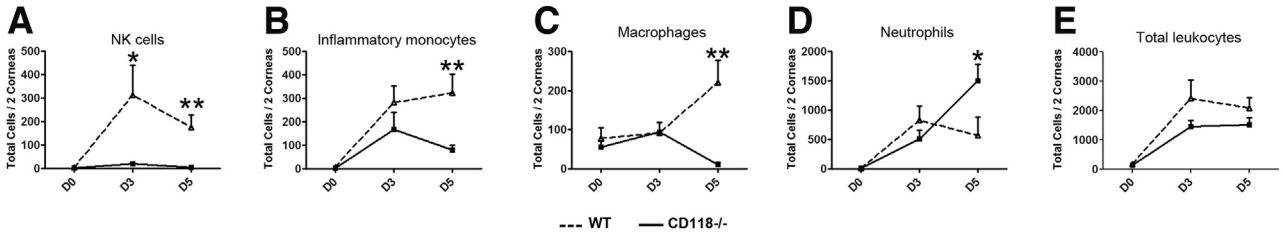


**Figure 3** HSV-1 infected *CD118*$^{-/-}$ mice have an altered leukocyte profile in the cornea proper. WT and *CD118*$^{-/-}$ mice were ocularly infected with $10^3$ PFU of HSV-1 or remained uninfected as controls (D0). On days 3 and 5 p.i. (D3 and D5, respectively), corneas were harvested, digested, and phenotyped by flow cytometry for NK cells (**A**), inflammatory monocytes (**B**), tissue macrophages (**C**), neutrophils (**D**), and CD45$^{Hi}$ total leukocytes (**E**). Results are presented as the means ± SEM of two to three experiments of two to four corneas per group per experiment. *$P < 0.05$, **$P < 0.01$ comparing WT with *CD118*$^{-/-}$ by unpaired *t*-test comparison.

Because changes in the influx of leukocytes were observed in the cornea of infected *CD118*$^{-/-}$ mice, one explanation could be reflected by changes in chemokine expression. As such, we examined CXCL1, CXCL9, and CXCL10 (Figure 4), all of which have been found to be expressed in the cornea of HSV-1-infected mice and/or influence the trafficking of monocytes and NK cells,[22,23] T cells,[24–27] and neutrophils.[28,29] The results showed an aberrant chemokine profile observed in the *CD118*$^{-/-}$ mouse corneas. Consistent with a reduction in the infiltration of NK cells and inflammatory monocytes, CXCL10 expression levels were significantly reduced on days 3 and 5 p.i. in the *CD118*$^{-/-}$ mouse corneas (Figure 4C). In contrast, there was a significant increase in CXCL1 expression by day 5 p.i. that correlated with a significant increase in the number of neutrophils residing in the tissue (Figure 4A). CXCL9 levels were not different between the *CD118*$^{-/-}$ and WT groups (Figure 4B).

## Loss of Lymphatic Vessels in the Cornea of *CD118*$^{-/-}$ Mice in Response to HSV-1

As previously shown, *CD118*$^{-/-}$ mouse corneas present as edematous with a noticeable increase in mass and unabated virus spread after infection (Figure 2). We propose that because HSV-1-driven lymphangiogenesis in the cornea requires virus-encoded ICP4 induction of VEGF-A expression[12] and *CD118*$^{-/-}$ mice possess a greater viral burden in the cornea, *CD118*$^{-/-}$ mice would display extensive lymphatic vessel development in comparison with WT mice. Indeed, this notion was found to be correct on day 3 p.i., wherein *CD118*$^{-/-}$ mice had significantly more LYVE-1$^+$ lymphatic vessel area (Figure 5, A and B). However, by day 5 p.i., the lymphatic vessels were absent in *CD118*$^{-/-}$ mice (Figure 5, A and B). The loss was selective for lymphatic endothelium because blood vessels remained intact (Figure 5A). Furthermore, infection of *CD118*$^{-/-}$ mice with GFP-expressing HSV-1 revealed localization of the virus in the peripheral cornea on day 5p.i., where lymphatic vessels previously existed (Supplemental Figure S1). To determine whether a tropism for LECs existed compared with BECs, human LEC and BEC were co-cultured *in vitro* and infected with GFP-expressing HSV-1. The percentage of HSV-1−positive LEC and BEC cells was similar, indicating equal susceptibility to infection *in vitro* (Figure 5C). This is in direct contrast to what was observed *in vivo*, wherein blood vessel integrity was maintained after infection, suggesting structural differences exist *in vivo* that protect blood vessels and not lymphatic vessels (Figure 5A). The data suggest unencumbered viral spread eventually results in the loss of lymphatic vessels in the cornea. To evaluate this possibility, WT mice were infected with an increasing inoculum of HSV-1. As seen in Figure 5D, WT mice infected with $10^6$ PFU display a diminution in lymphatic vessel integrity compared

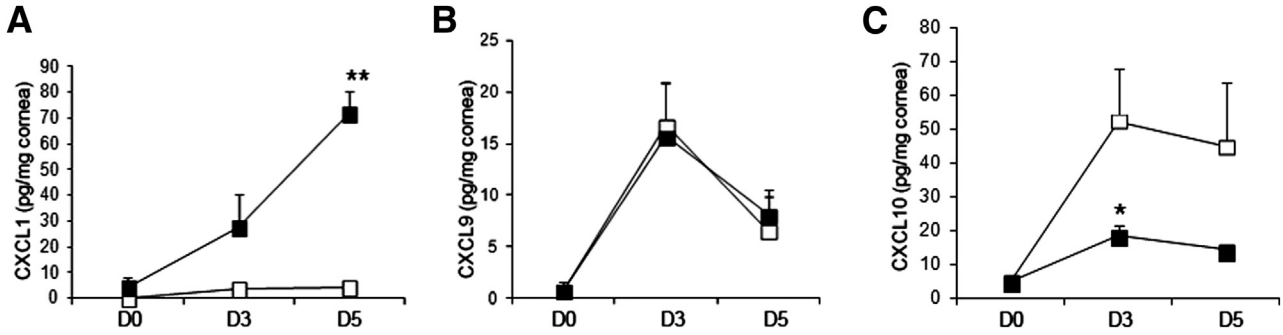


**Figure 4** The chemokine profile after HSV-1 infection is altered in the *CD118*$^{-/-}$ mouse cornea. WT (white boxes) and *CD118*$^{-/-}$ (black boxes) mice were ocularly infected with $10^3$ PFU of HSV-1 or remained uninfected as controls (D0). On days 3 and 5 p.i. (D3 and D5, respectively), corneas were harvested, homogenized, and processed for measurements of chemokines including CXCL1 (**A**), CXCL9 (**B**), and CXCL10 (**C**). Results are presented as pg/mg per cornea ± SEM of three independent experiments of two to three mice per group per experiment. *$P < 0.05$, **$P < 0.01$ comparing WT with *CD118*$^{-/-}$ by unpaired *t*-test comparison.

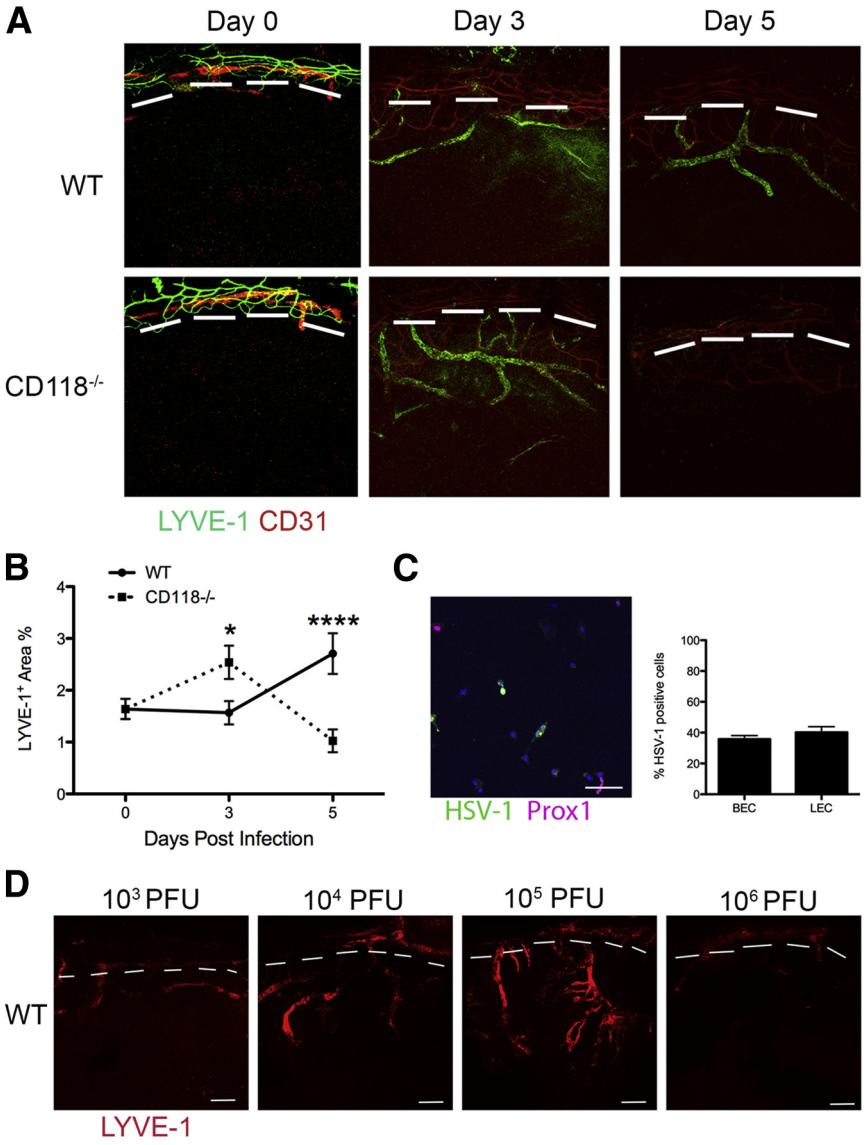


**Figure 5** Lymphangiogenesis after HSV-1 corneal infection in $CD118^{-/-}$ mice. **A**: LYVE-1 (green) and CD31 (red) expression in the cornea of WT mice and $CD118^{-/-}$ mice infected with$10^3$ PFU of HSV-1 on days 3 and 5 p.i. **B**: Lymphatic vessel area within the cornea proper were quantified and expressed as the percent area positive for LYVE-1 ($n = 4$ to 6 corneas per group per experiment). Error bars represent SEM. $^*P < 0.05$, $^{****}P < 0.0001$. Uninfected corneas (day 0) served as controls. **C**: LECs and BECs were co-cultured and infected with GFP-expressing HSV-1. Scale bars: 100 μm. Cells were subsequently stained for Prox1 expression. Cells positive for Prox1 (indicating LEC) or negative for Prox1 (indicating BEC) in the same visual field were counted as were the total cells (indicated by DAPI stain). The number of cells enumerated was then compared with the total number of cells in each visual field to calculate percentage of HSV-1—positive cells. Error bars represent SEM of 30 fields of view from two independent experiments. **D**: WT mice were infected with indicated PFU of HSV-1. On day 5 p.i., corneas were harvested and stained for LYVE-1 (red). Images are representative of two independent experiments with two to three mice per group. Scale bars: 200 μm. **White lines** show demarcation between the limbus and cornea proper.

with mice infected with $10^4$ PFU. Possible mechanisms for a reduction in lymphangiogenesis include reduced expression of pro-lymphangiogenic factors such as VEGF-A, VEGF-C, and VEGF-D. However, real-time RT-PCR analysis revealed an increase in both pro-angiogenic VEGF-A and VEGF-C gene expression in $CD118^{-/-}$ mice (Figure 6A). Furthermore, VEGF-A protein levels were also significantly elevated after HSV-1 infection of $CD118^{-/-}$ mice (Figure 6B). VEGF-C protein levels were not elevated above uninfected controls for either group (data not shown). Therefore, it would appear that the pro-angiogenic factor that drives lymphangiogenesis after HSV-1 infection, VEGF-A, was elevated in the $CD118^{-/-}$ mice compared with WT animals. Another possible explanation for a loss of lymphatic vessel genesis is the expression of the receptors that respond to the principal factor that drives HSV-1-induced lymphangiogenesis during acute infection, VEGFR2.[11] Analysis of VEGFR2 expression revealed no gross changes in expression comparing WT to $CD118^{-/-}$ mice (data not shown).

## Resident Cornea But not Hematopoietic-Derived Cells with a Functional Type I IFN Pathway Is Required to Maintain HSV-1—Induced Lymphatic Vessels

To further examine the targeting of lymphatic vessels by HSV-1, the contribution of resident (corneal stroma and epithelial cells) and bone marrow-derived cells (infiltrating leukocytes) was evaluated using $CD118^{-/-}$ and WT mouse chimeras. Cornea samples from WT mouse recipients of $CD118^{-/-}$ BM ($CD118^{-/-}$ BM>WT) and $CD118^{-/-}$ mouse recipients of WT BM (WTBM>$CD118^{-/-}$) possessed significantly more virus than WT mouse recipients of WT BM (WTBM>WT) indicating both resident cells and infiltrating leukocytes are important in viral surveillance in the cornea (Figure 7A). Lymphatic vessel genesis was preserved in mice in which the resident cell population possessed a fully competent type I IFN pathway (Figure 7, B and C). Taken together, these results suggest that in addition to virus and levels of the pro-angiogenic cytokines VEGF-A, VEGF-C, and VEGF-D,

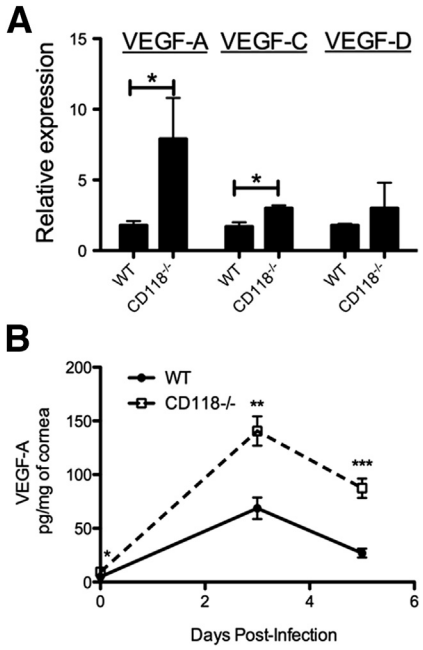


**Figure 6** HSV-1 infected *CD118*$^{-/-}$ mice are not deficient in VEGF-A or VEGF receptor 2 expression. **A:** Cornea levels of VEGF-A, VEGF-C, and VEGF-D were quantified by real-time RT-PCR and normalized to the housekeeping gene β-actin on day 5 p.i. ($n$ = 3 to 6 per group). **B:** VEGF-A levels in the cornea were determined by suspension array before and after HSV-1 infection of WT and *CD118*$^{-/-}$ mice ($n$ = 5 per group). Error bars represent SEM. *$P < 0.05$, **$P < 0.01$, ***$P < 0.0001$.

extraneous factors responsive to type I IFN signaling within resident cells facilitate the maintenance of lymphatic vessels within the cornea after HSV-1 infection.

### HSV-1 Infection in *CD118*$^{-/-}$ Mice Leads to a Loss of Resident Lymphatic Vessels in the Draining LN Resulting in Fluid Accumulation and Edema

The susceptibility of *CD118*$^{-/-}$ mice to ocular HSV-1 infection results in the dissemination of the virus to the draining MLN within 2 days p.i.[18] Because the virus is not detectable in the bloodstream until after day 5 p.i. in *CD118*$^{-/-}$ mice,[30] it is likely that the virus traffics to the MLN either directly or via resident dendritic cells that migrate via the lymphatics to the MLN after local CCL21 signaling. The result of localized MLN infection is reflected by a significant enlargement of the lymphoid tissue compared with WT animals (Figure 8A). The increase in weight is not due to the expansion of lymphoid cell numbers because the initial proliferation of cells is lost by day 5 p.i.[18] Rather, magnetic resonance imaging analysis revealed extensive edema in the MLN region of *CD118*$^{-/-}$ mice compared with WT mice (Figure 8, B and C). Similar to what is found in the cornea, we hypothesized that the destruction of LN lymphatic vessels by unhindered HSV-1 replication and spread may lead to fluid accumulation. Therefore, LN lymphatic vessels from infected WT and *CD118*$^{-/-}$ mice were visualized via confocal microscopy (Figure 8D). Quantification of LYVE-1-stained vessels revealed a significant reduction in the area occupied by lymphatic vessels in the *CD118*$^{-/-}$ mice compared with WT mice (Figure 8E). Consequently, the loss of lymphatic vessel occupancy in the MLN of *CD118*$^{-/-}$ mice corresponds with the edematous pathology likely due to i) an inability to drain the fluid via the efferent lymphatics as a result of discontinuity in the lymphatic structural system, ii) a structural blockage of the efferent lymphatics created by a massive loss of cells, or iii) a combination of the two events.

## Discussion

An unencumbered visual axis is due, in part, to the translucent nature of the avascular cornea and the immune-privileged environment established at the onset of ocular development that ultimately makes surgical procedures such as keratoplasty (cornea transplant) one of the most successful types of solid tissue transplantation.[31] However, a breach in the regulatory mechanisms that maintain this quiescent state, including trauma or infection, can have devastating results on visual acuity. To this end, the current study provides data

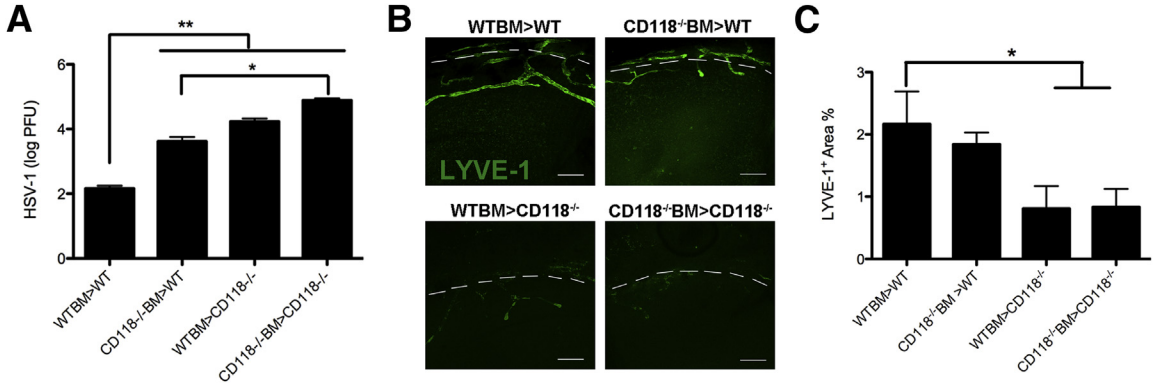


**Figure 7** Contribution of resident cells and infiltrating leukocytes to HSV-1 resistance and lymphangiogenesis. Mouse chimeras were infected with $10^3$ PFU of HSV-1. **A:** Corneas were harvested on day 5 p.i. and evaluated for viral titer by plaque assay ($n$ = 8 to 14 corneas per group). **B:** Corneas from infected mouse chimeras were stained for LYVE-1. Scale bars: 200 μm. **C:** Lymphatic vessel area within the cornea proper were quantified and expressed as the percent area positive for LYVE-1 ($n$ = 4 to 6 corneas per group per experiment). Error bars represent SEM. *$P < 0.05$, **$P < 0.01$.

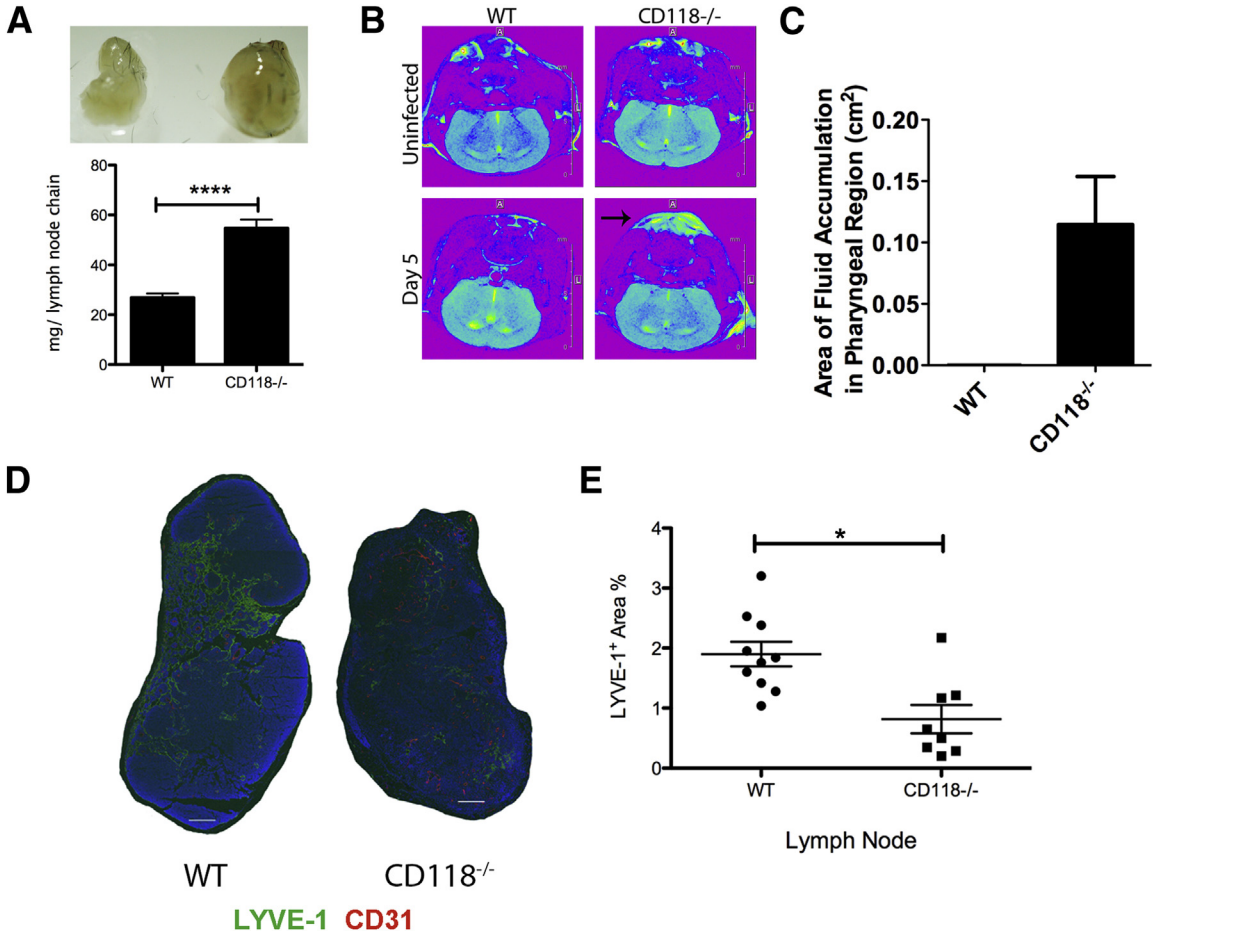


**Figure 8** Edema and selective loss of lymphatic vessels in the draining LNs. **A**–**E:** WT and *CD118*$^{-/-}$ mice were infected with $10^3$ PFU of HSV-1 and analyzed on day 5 p.i. **A:** Gross morphology and weight of WT and *CD118*$^{-/-}$ MLN chains ($n = 4$ to 6 per group). **B:** Mice were imaged using a Bruker Biospec (The Woodlands, TX) MRI imaging system to capture T2-weighted images. **C:** Areas of fluid accumulation were calculated by drawing regions of interest around the pharyngeal region and measured using Paravision software version 5.0 ($n = 3$ per group). **D:** Representative images of MLNs from WT and *CD118*$^{-/-}$ mice showing the distribution of LYVE-1$^+$ lymphatic vessels (green) and CD31$^+$ blood vessels (red). Scale bars: 200 μm. **E:** Lymphatic vessel area was quantified and expressed as the percent area positive for LYVE1 for the reconstructed LN images ($n = 6$ per group). One outlier for each group was identified and removed using a Grubb's test. *$P < 0.05$. ****$P < 0.0001$.

illustrating the cascade of events that transpire in the development of corneal pathology during acute HSV-1 infection that are exacerbated in the absence of a functional type I IFN pathway. The pathology comparing WT with *CD118*$^{-/-}$ mice are quite distinct. Although the HSV-1-infected WT mice presented with a relatively translucent cornea, the corneas of the infected *CD118*$^{-/-}$ mice were edematous with significant loss of epithelial cells. The epithelial defect was likely the result of virus replication due to the inability of *CD118*$^{-/-}$ mice to contain viral spread. In addition, epithelial cell loss and opacity may also be a consequence of the pronounced increase in neutrophil influx observed by day 5 p.i., along with the corresponding increase in matrix metalloproteinase-9 levels (data not shown).

In addition to neutrophils, other leukocyte populations residing in the cornea were found to be skewed between WT and *CD118*$^{-/-}$ mice. Specifically, NK cells, inflammatory monocytes, and macrophages were all elevated in the cornea of WT mice. Such results are consistent with the central role of inflammatory monocytes in HSV-1 surveillance in the cornea early during acute infection.[10] The recruitment of these cells includes expression of vascular addressins such as intercellular adhesion molecule 1 (ICAM-1), which were previously found to be necessary to manage ocular HSV-1[32] and chemokines.[33] Previously, we reported that the expression of CXCL10, but not CXCL9, was suppressed, whereas CXCL1 was elevated in the ganglion of *CD118*$^{-/-}$ mice after HSV-1 infection, similar to what is reported in the current study.[18] Whether the influx of immune cells into the cornea is directly related to this expression or due to additional chemokines and/or other factors is not resolved. Relative to CXCL1, we do know that the expression alone does not drive neutrophil influx into the cornea after HSV-1 infection, as determined using CXCL1-deficient mice.[34]

In the current study, we provide several unique examples of lymphatic vessel loss due to HSV-1 replication. In the context of HSV-1, low levels of the virus can promote lymphangiogenesis in the cornea; however, as the virus

replicates, lymphatic vessel integrity is compromised. The diminished presence of lymphatic vessels observed in the cornea of *CD118*$^{-/-}$ mice is not due to reduced expression of pro-lymphangiogenic factors or impaired leukocyte recruitment. *CD118*$^{-/-}$ and WT mouse chimeras revealed that the increased viral load alone does not account for lymphatic vessel loss. Rather, additional host factors that depend on type I IFN signaling must be required to maintain lymphatic signaling.

Ocular infection of *CD118*$^{-/-}$ mice with HSV-1 results in the rapid dissemination of the virus to the MLN as early as day 2 p.i.[18] Results from the current study indicate that the loss in LN lymphatics results in edema. The specific LN lymphatic vessels (cortical sinus, medullary sinus, or efferent lymphatic vessels) that are lost or compromised are currently unknown. During ocular HSV-1 infection, *CD118*$^{-/-}$ corneal lymphatics are destroyed by day 5 p.i. However, we predict that the lymphatic afferent vessels from other tissues will continue to drain into the MLN because lymphatic vessels are not completely lost in the draining LN and, therefore, some preservation of integrity is retained even in the presence of HSV-1.

LN lymphatic vessel destruction can occur via direct infection of LEC with HSV-1. However, we speculate that other factors may also contribute to the reduction of lymphatic vessels in MLN. Previous studies have shown that VEGF-A produced in chronically inflamed tissues can influence lymphangiogenesis in the downstream LN.[35] Nevertheless, the increased VEGF-A found in *CD118*$^{-/-}$ mouse corneas did not correlate with an increase in LN lymphangiogenesis. We propose that HSV-1 may modify the expression of several pro-lymphangiogenic factors by infecting various cell types within the MLN. Previous studies have indicated B cells and fibroblastic reticular cells as possible sources of VEGF-A within the inflamed LN.[36,37] Other important factors that could influence lymphangiogenesis include VEGF-C, fibroblast growth factor 2, and lymphotoxin alpha.[2] Furthermore, the destruction of LEC by HSV-1 may result in reduced CCL21 levels and subsequently the recruitment of CCR7$^{+}$ dendritic cells to the LN, thereby impairing the generation of an adaptive immune response.

Our initial experiments in the cornea and LN indicate that HSV-1 high viral titers can target lymphatic vessels resulting in tissue edema. We suspect the structural differences that exist between blood and lymphatic capillaries may account for the selective loss in lymphatic vessels within the cornea and MLN. Blood vessel endothelial cells form tight junctions and are surrounded by a basement membrane and layer of smooth muscle cells, whereas lymphatic capillaries lack a complete basement membrane and display gaps between endothelial cells.[1] Furthermore, previous work has suggested that the basement membrane restricts the spread of HSV.[38] With these findings, we propose a model for HSV-1 vesicle formation at low viral burdens, in which HSV-1 positively influences lymphangiogenesis through VEGF-A/VEGFR2 and fluid movement out of the infected tissue is unhindered. However, as the virus replicates locally to high concentrations, HSV-1 disrupts lymphatic, but not blood capillaries, through direct infection of LEC resulting in a loss of vessel integrity and fluid accumulation. This scenario may also function in the formation of skin vesicles or cold sores, one of the most common clinical manifestations of HSV-1 reactivation in the human population.

## Acknowledgments

We thank Drs. William P. Halford for the fluorescence expressing HSV-1 and Helen Rosenberg for the original *CD118*$^{-/-}$ mice.

K.M.B., A.J.C., C.D.C., A.C., and D.J.C. conceived and performed experiments, analyzed data, and were involved in the writing of the paper; M.Z. performed experiments.

## Supplemental Data

Supplemental material for this article can be found at *http://dx.doi.org/10.1016/j.ajpath.2013.06.014*.

## References

1. Karpanen T, Alitalo K: Molecular biology and pathology of lymphangiogenesis. Annu Rev Pathol 2008, 3:367–397
2. Shields JD: Lymphatics: at the interface of immunity, tolerance, and tumor metastasis. Microcirculation 2011, 18:517–531
3. Dietrich T, Bock F, Yuen D, Hos D, Bachmann BO, Zahn G, Wiegand S, Chen L, Cursiefen C: Cutting edge: lymphatic Vessels. Not blood vessels, primarily mediate immune rejections after transplantation. J Immunol 2010, 184:535–539
4. Chen L, Hamrah P, Cursiefen C, Zhang Q, Pytowski B, Streilein J, Dana M: Vascular ednothelial growth factor receptor-3 mediates induction of corneal alloimmunity. Nat Med 2004, 10:813–815
5. Howard M, Sellors JW, Jang D, Robinson NJ, Fearon M, Kaczorowski J, Chernesky M: Regional distribution of antibodies to herpes simplex virus type 1 (HSV-1) and HSV-2 in men and women in Ontario. Canada, J Clin Microbiol 2003, 41:84–89
6. Taylor T, Brockman M, McNamee E, Knipe D: Herpes simplex virus. Front Biosci 2002, 7:752–764
7. Rowe AM, St. Leger AJ, Jeon S, Dhaliwal DK, Knickelbein JE, Hendricks RL: Herpes keratitis. Prog Retin Eye Res 2012, 32:88–101
8. Bock F, Maruyama K, Regenfuss B, Hos D, Steven P, Heindl LM, Cursiefen C: Novel anti(lymph)angiogenic treatment for corneal and ocular surface diseases. Prog Retin Eye Res 2013, 34:89–124
9. Conrady CD, Zheng M, Fitzgerald KA, Liu C, Carr DJJ: Resistance to HSV-1 infection in the epithelium resides with the novel innate sensor, IFI-16. Mucosal Immunol 2012, 5:173–183
10. Conrady C, Zheng M, Mandal N, van Rooijen N, Carr D: IFN-α-driven CCL2 production recruits inflammatory monocytes to infection site in mice. Mucosal Immunol 2013, 6:45–55
11. Wuest TR, Carr DJJ: VEGF-A expression by HSV-1-infected cells drives corneal lymphangiogenesis. J Exp Med 2010, 207:101–115
12. Wuest T, Zheng M, Efstathiou S, Halford WP, Carr DJ: The herpes simplex virus-1 transactivator infected cell protein-4 drives VEGF-A dependent neovascularization. PLoS Pathog 2011, 7:e1002278
13. Suryawanshi A, Mulik S, Sharma S, Reddy PBJ, Sehrawat S, Rouse BT: ocular neovascularization caused by herpes simplex virus type 1 infection results from breakdown of binding between vascular

endothelial growth factor A and its soluble receptor. J Immunol 2011, 186:3653–3665
14. Garvey TL, Dyer KD, Ellis JA, Bonville CA, Foster B, Prussin C, Easton AJ, Domachowske JB, Rosenberg HF: Inflammatory responses to pneumovirus infection in IFN-alpha beta R gene-deleted mice. J Immunol 2005, 175:4735–4744
15. Liu M, Schmidt EE, Halford WP: ICP0 dismantles microtubule networks in herpes simplex virus-infected cells. PLoS ONE 2010, 5:e10975
16. Lively G, Jiang B, Hedberg-Buenz A, Chang B, Petersen G, Wang K, Kuehn M, Anderson M: Genetic dependence of central corneal thickness among inbred strains of mice. Invest Ophthalmol Vis Sci 2010, 51:160–171
17. Kataru R, Kim H, Jang C, Choi D, Koh B, Kim M, Gollamudi S, KIm Y, Lee S, Koh G: T lymphocytes negatively regulate lymph node lymphatic vessel formation. Immunity 2011, 34:96–107
18. Conrady CD, Thapa M, Wuest T, Carr DJJ: Loss of mandibular lymph node integrity is associated with an increase in sensitivity to HSV-1 infection in CD118-deficient mice. J Immunol 2009, 182:3678–3687
19. Cheng H, Tumpey TM, Staats HF, van Rooijen N, Oakes JE, Lausch RN: Role of macrophages in restricting herpes simplex virus type 1 growth after ocular infection. Invest Ophthalmol Vis Sci 2000, 41:1402–1409
20. Tumpey T, Chen S, Oakes J, Lausch R: Neutrophil-mediated suppression of virus replication after herpes simplex virus type 1 infection of the murine cornea. J Virol 1996, 70:898–904
21. Carr DJJ, Wuest T, Ash J: An increase in herpes simplex virus type 1 in the anterior segment of the eye is linked to a deficiency in N cell infiltration in mice deficient in CXCR3. J Interferon Cytokine Res 2008, 28:245–251
22. Luster AD: The role of chemokines in linking innate and adaptive immunity. Curr Opin Immunol 2002, 14:129–135
23. Carr DJJ, Tomanek L: Herpes simplex virus and the chemokines that mediate the inflammation. Curr Top Microbiol Immunol 2006, 303: 47–65
24. Himmelein S, St Leger AJ, Knickelbein J, Rowe A, Freeman M, Hendricks RL: Circulating herpes simplex type 1 (HSV-1)-specific CD8+ T cells do not access HSV-1 latently infected trigeminal ganglia. Herpesviridae 2011, 2:5
25. Wuest T, Farber J, Luster A, Carr DJJ: CD4+ T cell migration into the cornea is reduced in CXCL9 deficient but not CXCL10 deficient mice following herpes simplex virus type 1 infection. Cell Immunol 2006, 243:83–89
26. Groom J, Luster A: CXCR3 ligands: redundant, collaborative and antagonistic functions. Immunol Cell Biol 2011, 89:207–215
27. Groom JR, Luster AD: CXCR3 in T cell function. Exp Cell Res 2011, 317:620–631
28. Oquendo P, Alberta J, Wen DZ, Graycar JL, Derynck R, Stiles CD: The platelet-derived growth factor-inducible KC gene encodes a secretory protein related to platelet alpha-granule proteins. J Biol Chem 1989, 264:4133–4137
29. Yan XT, Tumpey TM, Kunkel SL, Oakes JE, Lausch RN: Role of MIP-2 in neutrophil migration and tissue injury in the herpes simplex virus-1-infected cornea. Invest Ophthalmol Vis Sci 1998, 39:1854–1862
30. Conrady CD, Zheng M, van Rooijen N, Drevets DA, Royer D, Alleman A, Carr DJ: Microglia and a functional type I IFN pathway are required to counter HSV-1-driven brain lateral ventricle enlargement and encephalitis. J Immunol 2013, 190:2807–2817
31. Niederkorn J: Immunology and immunomodulation of corneal transplantation. Int Rev Immunol 2002, 21:173–196
32. Noisakran S, Härle P, Carr DJJ: ICAM-1 is required for resistance to herpes simplex virus type 1 but not interferon-α1 transgene efficacy. Virology 2001, 283:69–77
33. Araki-Sasaki K, Tanaka T, Ebisuno Y, Kanda H, Umemoto E, Hayashi K, Miyasaka M: Dynamic expression of chemokines and the infiltration of inflammatory cells in the HSV-infected cornea and its associated tissues. Ocul Immunol Inflamm 2006, 14:257–266
34. Bryant-Hudson KM, Carr DJJ: CXCL1-deficient mice are highly sensitive to pseudomonas aeruginosa but not herpes simplex virus type 1 corneal infection. Invest Ophthalmol Vis Sci 2012, 53:6785–6792
35. Halin C, Tobler NE, Vigl B, Brown LF, Detmar M: VEGF-A produced by chronically inflamed tissue induces lymphangiogenesis in draining lymph nodes. Blood 2007, 110:3158–3167
36. Tan KW, Yeo KP, Wong FHS, Lim HY, Khoo KL, Abastado J-P, Angeli Vr: Expansion of cortical and medullary sinuses restrains lymph node hypertrophy during prolonged inflammation. J Immunol 2012, 188:4065–4080
37. Angeli V, Ginhoux F, Llodra J, Quemeneur L, Frenette PS, Skobe M, Jessberger R, Merad M, Randolph GJ: B cell-driven lymphangiogenesis in inflamed lymph nodes enhances dendritic cell mobilization. Immunity 2006, 24:203–215
38. Weeks BS, Ramchandran RS, Hopkins JJ, Friedman HM: Herpes simplex virus type- 1 and 2 pathogenesis is restricted by the epidermal basement membrane. Arch Virol 2000, 145:385–396